

Anisotropic Structure Deformation in the VO₂ Metal-Insulator Transition

Jamie M. Booth and Philip S. Casey

CSIRO Materials Science and Engineering, Private Bag 33, Clayton South, 3169, Victoria, Australia

(Received 12 May 2009; published 18 August 2009)

X-ray absorption fine structure data of tungsten (VI)-doped vanadium dioxide in the insulating phase, and during the metal-insulator transition, are presented for the first time. Tungsten *L*_{III}- and vanadium *K*-edge data suggest that significant expansion in the [110] and [$\bar{1}\bar{1}0$] directions occurs across the phase transition from low to high temperature. This distortion breaks the bonds between Peierls-paired vanadium ions, opening a band gap, and reveals the nature of the mechanism by which tungsten doping lowers the transition temperature and enthalpy.

DOI: 10.1103/PhysRevLett.103.086402

PACS numbers: 71.30.+h, 71.27.+a

The origin of the driving force(s) behind the metal-insulator transition (MIT) of VO₂ has been something of a mystery for decades. The transition is characterized by a crystal structure change from high-temperature tetragonal $P4_2/mnm$ (136)—the rutile structure—to a low-temperature monoclinic $P2_1/c$ (12) at 340 K corresponding to V⁴⁺ cations along the rutile *c* axis forming homopolar bonds, and undergoing a structural twist [1,2] (see Fig. 1). This decrease in symmetry and the creation of a bonding-antibonding pair result in a band gap opening. Such a structural change is characteristic of a Peierls-type transition in that it seems to be totally structurally driven, however, there is also considerable evidence for what is seen as a competing mechanism. In a Mott-type MIT the band gap opens due to strong electron-electron correlations rather than phonon or electron-phonon interaction contributions. While the crystal structure change of VO₂ suggests that the MIT is the result of phonon mode softening, a perspective which is supported by both experimental data [3,4] and computational work [5–7], the divergence of the quasiparticle mass in particular, as the structure changes from high to low symmetry, points to the significant role played by electron correlations [8,9]. Both mechanisms therefore have voluminous amounts of theoretical and experimental evidence [1], and in recent times this has led to the recognition that both mechanisms are active and the transition is viewed as a Mott-assisted Peierls MIT, and vice versa [8,10–12].

However, the exact interplay of the two mechanisms is still a subject of considerable debate. Specifically, the unresolved question seems to be, How can a Peierls (Mott) mechanism generate the behavior characteristic of a Mott (Peierls) MIT?

In this Letter we present x-ray absorption fine structure (XAFS) spectrometry data on tungsten-doped VO₂ in an attempt to gain new insight into the nature of the MIT by investigating, for the first time, the local structure of both vanadium and tungsten below and during the transition. It is well known that the introduction of dopants can have a significant effect on the MIT of VO₂. Tungsten (VI) in

particular has received much practical attention due to its lowering of the transition temperature by approximately 23–26 K/dopant percent [13–16], while Cr(VI) has received similar attention from theorists due to its role in the formation of the transitional $C2/m M_2$ structure [17,18].

We find that the influence of the W⁶⁺ dopant on the local structure manifests as the formation of regions of tetragonal symmetry, which propagate through corner sharing to neighboring unit cells, while stress through the apical oxygens propagates to the neighboring sublattices, resulting in a strain on the V-V homopolar bonds. This and the vanadium *K*-edge data of a sample undergoing its MIT provide convincing evidence that the MIT is structurally driven: approaching the transition from low temperature results in

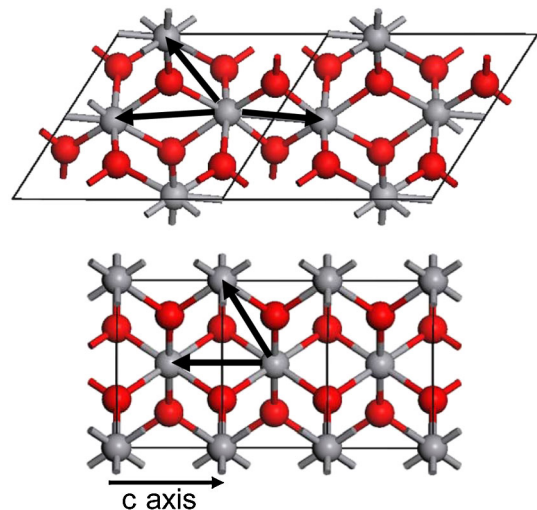


FIG. 1 (color online). Identical perspectives of the low-temperature monoclinic structure (top) and the high-temperature tetragonal structure of VO₂ (bottom), showing the Peierls pairing and the slight twist of the V(IV) ions (light gray) in the monoclinic form along the equivalent of the tetragonal *c* axis. Important vanadium-vanadium XAFS scattering distances are marked with arrows.

significant expansion of the crystal structure in the $[110]_R$ and $[1\bar{1}0]_R$ directions of the rutile unit cell which (to the best of our knowledge) has no literary precedent. The expansion strains the V-V homopolar bonds of the neighboring sublattice, in the same manner as an externally applied uniaxial stress was found to [19], causing them to break. We postulate that the close proximity of the resultant metallic doublets of the $d_{x^2-y^2}$ orbitals, in what may be a correlated metal species [20], results in scattering which modifies the quasiparticle masses and lifetimes.

Tungsten-doped VO_2 powders were prepared by reacting aspartic acid with V_2O_5 in aqueous solution in the presence of the required amount of Na_2WO_4 [21] to produce 0.5%, 1.0%, and 1.9% W-doped samples. The resultant amorphous product was calcined under argon at either 800 °C for 8 hours in the case of the 0.5% doped sample or both 800 °C and 950 °C for 8 hours each for the 1.0% and 1.9% doped samples. X-ray diffraction was used to characterize the phase homogeneity, and the phase transition characteristics of transition temperature and enthalpy were confirmed with differential scanning calorimetry. XAFS data at the tungsten L_{III} and vanadium K edges were obtained in fluorescence mode at ambient temperature (24 °C) on beam line 20B at the Photon Factory in Tsukuba, Japan.

Vanadium K -edge data in R space of a 1% doped sample of VO_2 well below its MIT [Fig. 2(a)] were fitted with both the monoclinic and tetragonal structures using the program ARTEMIS. The V-V1, V-V2, and V-V3 distances are only in good agreement with those calculated for the monoclinic structure, although the magnitudes of the peaks are a less complete match, and the multiple k weighting used in the fitting procedure resolves the V-V2 peak more clearly with respect to the experimental data, which are k^3 weighted only. The tungsten L_{III} -edge data, however [Fig. 2(b)], manifest very different characteristic distances. The R -space data match very closely those obtained by Tang *et al.* [13] for 5% tungsten-doped VO_2 at the W L_{III} edge, with strong peaks at 1.47 Å, 2.77 Å, and 3.22 Å corresponding to W-O, W-V1, and W-V2 scattering paths, respectively. The W-V1 peak expected from a monoclinic structure around the tungsten core is completely missing; instead the spectrum manifests only two W-V distances in the range 2–4 Å.

This symmetry is characteristic of a tetragonal structure, and in a recent computational study [7], it was predicted that the local environment of tungsten dopant in the low-temperature phase is approximated by that of vanadium in the high-temperature phase. Replacing the vanadium core in the tetragonal FEFF input file with tungsten resulted in a good fit to the first two shells, a Jahn-Teller distorted doubly degenerate oxygen shell, and a fourfold degenerate oxygen shell, although the fit for longer paths was again poor. Fitting the data between $2 \text{ \AA} < r < 4 \text{ \AA}$ with only those paths calculated to fall within this range shows a good fit for the W-V1 and W-V2 distances, confirming that

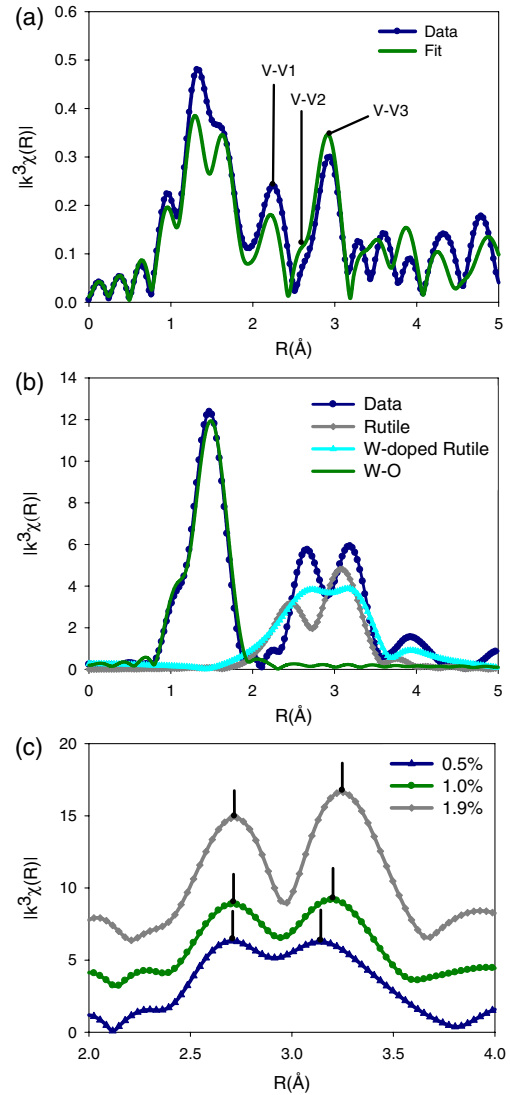


FIG. 2 (color online). (a) Vanadium K -edge XAFS data in R space of a 1% W-doped VO_2 sample (blue line with dots) in the insulating state, with the corresponding multiple k -weight fit using the M_1 structure (green line). (b) Fourier transform of the k^3 -weighted W L_{III} -edge data of a 1% doped W-doped VO_2 sample below the MIT fitted independently with the first two Jahn-Teller distorted oxygen shells with a W L_{III} hole, the VO_2 rutile structure from 2 to 4 Å with a V K hole, and the rutile structure from 2 to 4 Å with a W L_{III} hole. (c) Fourier transform of the k^3 -weighted W L_{III} data of three samples of 0.5%, 1.0%, and 1.9% W-doped VO_2 between 2 and 4 Å, showing the static W-V1 distance, and increasing W-V2 distance as a function of dopant loading.

the local environment of the dopant is that of a rutile structure. A comparison of Figs. 2(a) and 2(c) also suggests that the rutile structure around the dopant results in a longer scattering path to the V3 ion of the monoclinic structure. Therefore, as predicted computationally [7], the structure observed not only exhibits higher symmetry but also an increase in cationic spacing.

The adoption of this symmetry is unsurprising, as the dopant added was a W^{6+} species, and has no valence electrons with which to bond to neighboring vanadium cations. The shorter Peierls pairing distance is therefore not expected, and the two closest V^{4+} cations will be arranged symmetrically around the tungsten. This W^{6+} dopant will also not donate any electrons to neighboring vanadium cations, as postulated for a W^{4+} dopant [13], and it cannot activate the insulating phase via charge compensation since V^{4+} already has a partially filled band. Therefore its influence on neighboring cells will be structural in nature only. This influence becomes more pronounced upon further doping, as Fig. 2(c) demonstrates. Increasing the dopant loading from 0.5%, to 1%, to 1.9% results in increasing resolution between the W-V1 and W-V2 peaks, suggesting expansion of the rutile unit cell structure around the tungsten core. However, closer inspection of the peaks shows that the W-V1 distance remains static, and only the W-V2 distance is increasing. This suggests that the expansion has no component in the c axis of the rutile cell. The structural distortion is therefore in the $[110]_R$ and $[1\bar{1}0]_R$ directions.

Many years ago Pouget *et al.* [19] applied uniaxial stresses along the $[110]_R$ direction of pure VO_2 samples and found that this induced depairing of the homopolar bonded vanadium ions in one of the two sublattices, as the stress will propagate through the apical oxygens and result in a strain on the V-V bond, decreasing $d_{||}$ orbital overlap. This results in the formation of the transitional M_2 structure, in which only half of the Peierls pairings are broken. This work, combined with the well-known facilitation of the phase transition by tungsten, and the experimental data suggest that a similar mechanism is occurring in W-doped VO_2 . In this case, the strain will occur on both sublattices, as the XAFS data indicate that the expansion is in both directions; otherwise the W-V2 peak would split, and this is not observed. Corner sharing of the vanadium ions with respect to the rutile cell will result in the expansion propagating to neighboring cells along the c axis. The dopant therefore results in the transfer of strain to the V-V bonds in the neighboring sublattice through its own and neighboring unit cells along the c axis, which suggests the creation of nucleation sites for the MIT. Also of note is the higher symmetry of the oxygen octahedral coordination around the tungsten in comparison to the vanadium, indicating that the oxygens are arranged in the higher symmetry form of the rutile cell, rather than the distorted octahedron expected for the monoclinic phase.

This expansion is echoed in the vanadium K -edge data of a sample undergoing its MIT (Fig. 3). This sample was doped with 1.9% tungsten, and experiences a sharp first order phase transition at 23.3 °C [21] and is compared to a 1% W-doped sample which is well below its MIT. The V-O scattering paths show much greater overlap, analogous to the W L_{III} data, indicating greater symmetry of the oxygens about the vanadium. This increased symmetry decreases V_d-O_p hybridization, lowering the energy of the

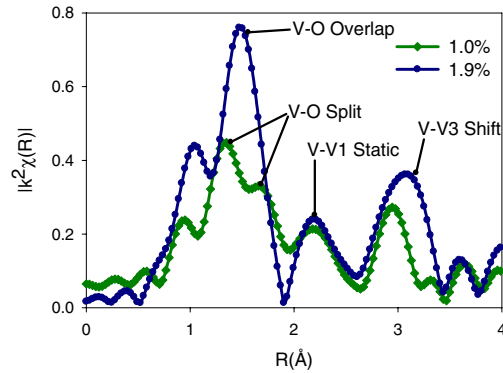


FIG. 3 (color online). Vanadium K -edge data of a 1% doped sample below its MIT juxtaposed with a 1.9% doped sample undergoing its MIT.

π^* bands. The increase in V-V3 distance, which is analogous to the W-V2 distance, is also observed, indicating that like the doped unit cells well below the MIT, the undoped cells experience expansion towards the corners of the rutile cell. However, the peak well below the phase transition is a combination of the V-V2 and V-V3 peaks, while the peak in the transitional structure shows splitting, indicating that the V-V2 peak is static while the V-V3 peak shifts, again illustrating that the expansion has no c component (due to the static V-V2 distance) and is therefore in the $[110]_R$ and $[1\bar{1}0]_R$ directions.

Of particular note is the static V-V1 peak of the Peierls-paired vanadium ions, which does not show a change in intensity, indicating that the expansion of the unit cell orthogonal to the c axis occurs before the V-V bonds break. Fitting of the spectrum with the transitional $C2/m$ M_2 structure [1] showed very poor correlation. This is almost certainly due to the fact that the M_2 structure does not show the expansion in the $[110]_R$ and $[1\bar{1}0]_R$ directions of the experimental data. Additionally, in the M_2 structure the V-V bonds on one of the sublattices are broken, and thus it is V-V1 which changes, as half of the V-V1 distances become V-V2 paths. Therefore in the transitional state of Fig. 2(a) the V-V3 paths manifest at too high a path length, while the intensities of the V-V1 and V-V2 peaks are a very poor match to the M_2 structure. This does not preclude the formation of the M_2 structure as a transitional state, however, once the V-V bonds begin to break, although more recent work [22] suggests that the MIT occurs without passing through the M_2 structure. These data are convincing evidence that it is the expansion which causes V-V bond cleavage due to decreasing $d_{||}$ orbital overlap, and not the converse.

The XAFS data therefore indicate that in going from an insulator to a metal, the VO_2 structure shows an expansion in the $[110]_R$ and $[1\bar{1}0]_R$ directions. This is accompanied by “detwisting” of the vanadium octahedra, indicated by reduced distortion manifesting as increasing symmetry of the V-O distances. This expansion will propagate through the apical oxygens of the octahedra to the neighboring

sublattice, inducing a strain on the V-V homopolar bonds of the c axis, decreasing orbital overlap and resulting in depairing of the vanadium ions. Because of the biaxial nature of the expansion, the strain is experienced by both sublattices in the M_1 structure, and any formation of the M_2 structure will be transitional, as both sublattices will experience V-V depairing. The structural bottleneck observed in ultrafast microscopy experiments [4] may therefore be the detwisted, higher symmetry structure of Fig. 3, before the V-V bonds break.

Such distortion is supported by the calculations of Gervais and Kress [5], who found a softening of the rutile structure at the R point, and the phonon eigenvectors of the lowest frequency mode are exactly those that would manifest if the above structural transition was reversed. Therefore the experimental data presented here combined with computational work [5–7] suggest that the driving force for the unit cell expansion is phonon hardening.

Given that two lobes of the vanadium $d_{x^2-y^2}$ orbitals are oriented along the rutile c axis [1], as the unit cell contracts (expands) along this axis the increasing (decreasing) proximities of the orbitals will result in increasing (decreasing) scattering which contributes to the self-energy, which is related to the Green's function (propagator) [23] by the Dyson equation:

$$G = G_0 + G_0 \Sigma G, \quad (1)$$

where G_0 and G are the bare and dressed propagators, respectively, and Σ is the self-energy. This change in self-energy modifies the renormalized quasiparticle density of states and therefore the quasiparticle mass [23]. Therefore, in concert with the structural distortion from low frequency phonon mode softening [5–7], changes in quasiparticle mass and lifetime are expected which may explain the divergent effective mass with decreasing temperature observed by other authors [8,9].

The giant transfer of spectral weight across the transition [11] is recognized as the breaking of the V-V bond, resulting in a charge redistribution around the V ions, which becomes more isotropic. The transitions to the antibonding $d_{||}$ orbital disappear above the MIT, as the bonding-antibonding pair is destroyed, and the $d_{||}$ gap closes. The observation that the orbital switching upon cooling can only be made if the system is close to a Mott insulating [8,10] regime is also consistent with the interpretation above, as electron scattering will be induced before Peierls pairing occurs. The picture of areas of high lattice distortion induced by temperature (and by tungsten doping) and resulting in high localized strains on V-V bonds is consistent with metallic nanopuddle behavior [9], as the V sites will act as nuclei for the puddles, which eventually percolate, and the material completely transforms.

The puzzling trend of decreasing enthalpy with decreasing phase transition temperature in W-doped VO₂ can also now be explained [15,21]. The inserted dopant causes lattice deformations towards the high-temperature structure which reduce the amount of work which must be done

across the phase transition. The energy required therefore lowers as dopant amount increases. This also suggests that the amount of energy needed to successfully dope the structure will increase with increasing dopant loading, which has been noticed during some syntheses [21].

The authors would like to gratefully acknowledge funding and assistance from the Australian National Beamline Facility.

-
- [1] V. Eyert, Ann. Phys. (Leipzig) **11**, 650 (2002).
 - [2] J. B. Goodenough, J. Solid State Chem. **3**, 490 (1971).
 - [3] D. B. McWhan, M. Marezio, J. P. Remeika, and P. D. Dernier, Phys. Rev. B **10**, 490 (1974).
 - [4] A. Cavalleri, Th. Dekorsy, H. H. W. Chong, J. C. Kieffer, and R. W. Schoenlein, Phys. Rev. B **70**, 161102(R) (2004).
 - [5] F. Gervais and W. Kress, Phys. Rev. B **31**, 4809 (1985).
 - [6] S. M. Woodley, Chem. Phys. Lett. **453**, 167 (2008).
 - [7] M. Netsianda, P. E. Ngoepe, C. R. A. Catlow, and S. Woodley, Chem. Mater. **20**, 1764 (2008).
 - [8] S. Biermann, A. Poteryaev, A. I. Lichtenstein, and A. Georges, Phys. Rev. Lett. **94**, 026404 (2005).
 - [9] M. M. Qazilbash, M. Brehm, B.-G. Chae, P.-C. Ho, G. O. Adreev, B.-J. Kim, S. J. Yun, A. V. Balatsky, M. B. Maple, F. Keilmann, H.-T. Kim, D. N. Basov, Science **318**, 1750 (2007).
 - [10] M. W. Haverkort, Z. Hu, A. Tanaka, W. Reichelt, S. V. Streltsov, M. A. Korotin, V. I. Anisimov, H. H. Hsieh, H.-J. Lin, C. T. Chen, D. I. Khomskii, and L. H. Tjeng, Phys. Rev. Lett. **95**, 196404 (2005).
 - [11] T. C. Koethe, Z. Hu, M. W. Haverkort, C. Schüssler-Langeheine, F. Venturini, N. B. Brookes, O. Tjernberg, W. Reichelt, H. H. Hsieh, H.-J. Lin, C. T. Chen, and L. H. Tjeng, Phys. Rev. Lett. **97**, 116402 (2006).
 - [12] J. M. Tomczak, F. Aryasetiawan, and S. Biermann, Phys. Rev. B **78**, 115103 (2008).
 - [13] C. Tang, P. Georgopoulos, M. E. Fine, J. B. Cohen, M. Nygren, G. S. Knapp, and A. Aldred, Phys. Rev. B **31**, 1000 (1985).
 - [14] T. D. Manning, I. P. Parkin, M. E. Pemble, D. Sheel, and D. Vernadou, Chem. Mater. **16**, 744 (2004).
 - [15] J. Shi, S. Zhou, B. You, and L. Wu, Solar Energy Mater. Sol. Cells **91**, 1856 (2007).
 - [16] Z. Peng, W. Jiang, and H. Liu, J. Phys. Chem. C **111**, 1119 (2007).
 - [17] A. Zylberstejn and N. F. Mott, Phys. Rev. B **11**, 4383 (1975).
 - [18] J. P. Pouget and H. Launois, J. Phys. (Paris) **37**, C4-49 (1976).
 - [19] J. P. Pouget, H. Launois, J. P. D'Haenens, P. Merenda, and T. M. Rice, Phys. Rev. Lett. **35**, 873 (1975).
 - [20] M. M. Qazilbash, K. S. Burch, D. Whisler, D. Shrekenhamer, B. G. Chae, H. T. Kim, and D. N. Basov, Phys. Rev. B **74**, 205118 (2006).
 - [21] J. M. Booth, P. S. Casey, and W. Yang (to be published).
 - [22] H.-T. Kim, Y. W. Lee, B.-J. Kim, B.-G. Chae, S. J. Yun, K.-Y. Kang, K.-J. Han, K.-J. Yee, and Y.-S. Lim, Phys. Rev. Lett. **97**, 266401 (2006).
 - [23] M. Imada, A. Fujimori, and Y. Tokura, Rev. Mod. Phys. **70**, 1039 (1998).